

Scalable Evaluation of Hadamard Products with Tensor Product Basis for Entropy-Stable High-Order Methods

Alexander Cicchino^{a,1,*}, Siva Nadarajah^{a,2}

^a*Department of Mechanical Engineering, McGill University, Montreal, QC, H3A 0C3, Canada*

Abstract

Keywords: Sum-Factorization, Hadamard Product, Entropy Conserving, Discontinuous Galerkin, Flux Reconstruction

1. Introduction

Sum-Factorization techniques were introduced by Orzag [1] to efficiently evaluate spectral methods. Orzag [1] made use of the tensor product nature of the basis functions to perform the operations in each direction independently, and result in $\mathcal{O}(n^{d+1})$ flops for interpolation, projection and differentiation operations. Unfortunately, a tensor product algorithm resulting in $\mathcal{O}(n^{d+1})$ flops for Hadamard products does not yet exist in the literature. The aim of this technical note is to demonstrate that Hadamard products can be computed in $\mathcal{O}(n^{d+1})$ flops with a tensor product basis, provided the basis functions have one additional property that is common in the spectral and finite element communities.

Entropy stable numerical schemes, initially proposed by Tadmor [2] for finite-volume methods, guarantee robustness on extremely coarse meshes. Through the application of summation-by-parts (SBP) operators, and introducing flux differencing techniques, Fisher *et al.* [3, 4] made the concepts from Tadmor applicable in a finite-element framework. This led to the development of provably nonlinearly stable high-order methods [3–15], in a collocated split-form discontinuous Galerkin (DG) form [16, 17], collocated split-form flux reconstruction (FR) framework recovering the DG case [18–20], modal, uncollocated entropy stable DG framework [21–24], and modal, uncollocated nonlinearly stable FR (NSFR) schemes [25, 26].

*Corresponding author.

Email addresses: alexander.cicchino@mail.mcgill.ca (Alexander Cicchino), siva.nadarajah@mcgill.ca (Siva Nadarajah)

¹Ph.D. Student

²Professor

In the application of flux differencing [3, Eq. (3.9)], Ranocha *et al.* [27] numerically demonstrated that $\mathcal{O}(n^{d+1})$ flops could be recovered. For modal, uncollocated schemes, the general expression requires the computation of a dense Hadamard product, as seen in Chan [21, Eq. (58)]. The focus of this short note is on efficiently evaluating a Hadamard product using a tensor product basis. Specifically, using the tensor product structure, we demonstrate that a Hadamard product can be assembled and evaluated in $\mathcal{O}(n^{d+1})$ flops and memory allocation, rather than $\mathcal{O}(n^{2d})$, where d is the dimension. We term the algorithm a “sum-factorized” Hadamard product because we recover the scaling result of sum-factorization techniques [1] by exploiting the tensor-product structure in the Hadamard product. This result is dependent on the basis operators being diagonal operators in at least $d - 1$ directions—fortunately this is always the case for Hadamard products involving interpolation, projection and differentiation operators of polynomial basis functions. This is the case because we can use sum-factorization techniques to project onto a collocated Lagrange basis, evaluate the Hadamard product using our proposed algorithm, then project back onto the dense basis. In Section 3, we provide numerical results showing that the Hadamard product scales at $\mathcal{O}(n^{d+1})$. Then we numerically show the application in our in-house partial differential equation solver PHILIP [28] based on the Nonlinearly Stable Flux Reconstruction scheme [25, 26] and demonstrate that the entire solver scales at $\mathcal{O}(n^{d+1})$ for three-dimensional compressible flow on curvilinear grids, in a low-storage manner. Lastly, we compare the computational costs between a conservative strong form DG scheme, an over-integrated conservative strong form DG scheme, and our NSFR entropy conserving scheme. The NSFR entropy conserving scheme is the only scheme that requires a dense Hadamard product evaluation. We numerically demonstrate that with our proposed sum-factorized Hadamard products, the NSFR entropy conserving scheme is computationally competitive with the DG conservative strong form, and that over-integration schemes take significantly more computational time.

2. Hadamard Product

Consider solving $(\mathbf{A} \otimes \mathbf{B}) \circ \mathbf{C}$, with $\mathbf{A}, \mathbf{B} \in \mathbb{R}^{n \times n}$ and $\mathbf{C} \in \mathbb{R}^{n^2 \times n^2}$.

$$(\mathbf{A} \otimes \mathbf{B}) \circ \mathbf{C} = \begin{bmatrix} A_{11} [\mathbf{B} \circ \mathbf{C}_{11}] & \dots & A_{1n} [\mathbf{B} \circ \mathbf{C}_{1n}] \\ \vdots & \vdots & \vdots \\ A_{n1} [\mathbf{B} \circ \mathbf{C}_{n1}] & \dots & A_{nn} [\mathbf{B} \circ \mathbf{C}_{nn}] \end{bmatrix}. \quad (1)$$

The computational cost associated with solving the Hadamard product in Eq. (1) is $\mathcal{O}(n^4)$. Unfortunately, unlike sum-factorization [1], it is not possible to reduce the computational cost of Eq. (1) by evaluating each

direction independently.

If we add an additional condition, $\mathbf{A} = \text{diag}(\mathbf{a})$, $\mathbf{a} \in \mathbb{R}^{n \times 1}$, then

$$(\mathbf{A} \otimes \mathbf{B}) \circ \mathbf{C} = \begin{bmatrix} a_1 [\mathbf{B} \circ \mathbf{C}_{11}] & & 0 \\ & \ddots & \\ 0 & & a_n [\mathbf{B} \circ \mathbf{C}_{nn}] \end{bmatrix} = \text{diag} \begin{pmatrix} a_1 [\mathbf{B} \circ \mathbf{C}_{11}] \\ \vdots \\ a_n [\mathbf{B} \circ \mathbf{C}_{nn}] \end{pmatrix}_{n^2 \times n}. \quad (2)$$

The computational cost to evaluate Eq. (2) is $O(n^3)$. Similarly, if $\mathbf{B} = \text{diag}(\mathbf{b})$ with \mathbf{A} dense, then $(\mathbf{A} \otimes \mathbf{B}) \circ \mathbf{C}$ costs $O(n^3)$ to evaluate by changing the stride through the matrix.

This can be generalized for an arbitrary d -sized tensor product, $(\mathbf{A}_1 \otimes \mathbf{A}_2 \otimes \cdots \otimes \mathbf{A}_d) \circ \mathbf{C}$, with $\mathbf{A}_1, \dots, \mathbf{A}_d \in \mathbb{R}^{n \times n}$ and $\mathbf{C} \in \mathbb{R}^{n^d \times n^d}$. If $\mathbf{A}_i = \text{diag}(\mathbf{a}_i)$, $\mathbf{a} \in \mathbb{R}^{n \times 1}$, $\forall i = 1, \dots, d-1$, then,

$$(\mathbf{A}_1 \otimes \mathbf{A}_2 \otimes \cdots \otimes \mathbf{A}_d) \circ \mathbf{C} = \text{diag} \begin{pmatrix} (\mathbf{a}_1)_1 \dots (\mathbf{a}_{d-1})_1 [\mathbf{A}_d \circ \mathbf{C}_{11}] \\ \vdots \\ (\mathbf{a}_1)_n \dots (\mathbf{a}_{d-1})_n [\mathbf{A}_d \circ \mathbf{C}_{n^d n^d}] \end{pmatrix}_{n^d \times n^d}, \quad (3)$$

and similarly for the other $d-1$ directions through pivoting. Thus, in each of these d -cases, the total computational cost is $dn^{d+1} = O(n^{d+1})$, $\forall n \gg d$.

In the context of high-order entropy stable methods, the Hadamard product can always be computed with the diagonal property above, regardless of the basis functions. Consider solving,

$$\left(\frac{\partial \chi(\xi_v^r)}{\partial \xi_j^\alpha} \mathbf{\Pi} \right) \circ \mathbf{C}, \quad (4)$$

where χ is some linearly independent, polynomial basis, ξ_v^r are a set of nodes that the basis are evaluated on in computational space, ξ_j is a direction that the α -th order derivative is applied in, and $\mathbf{\Pi}$ is the projection operator corresponding to the basis χ such that $\mathbf{\Pi}\chi(\xi_v^r) = \mathbf{I}$. Using Zwanenburg and Nadarajah [29, Proposition 2.1 and Corollary 2.2], we can always make the substitution $\frac{\partial^\alpha \chi(\xi_v^r)}{\partial \xi_j^\alpha} = \frac{\partial^\alpha \ell(\xi_v^r)}{\partial \xi_j^\alpha} \mathbf{\Pi}$ where ℓ is the Lagrange basis collocated on the nodes ξ_v^r —that is $\ell(\xi_v^r) = \mathbf{I}$. If we let ℓ be a tensor product basis, then $\frac{\partial^\alpha \ell(\xi_v^r)}{\partial \xi_j^\alpha} = \mathbf{I}(\xi_{i < j}) \otimes \frac{d^\alpha \ell(\xi_j)}{d \xi_j^\alpha} \otimes \mathbf{I}(\xi_{i > j})$. Therefore, $\frac{\partial^\alpha \chi(\xi_v^r)}{\partial \xi_j^\alpha} \circ \mathbf{C}$ recovers the form of Eq. (3), where $\mathbf{A}_i = \mathbf{I} \forall i = 1, \dots, d$, $i \neq j$. Similarly, if we have some weight function that is a non-identity diagonal matrix multiplied to the derivative, then we have,

$$\mathbf{W}(\xi_v^r) \left(\frac{\partial \chi(\xi_v^r)}{\partial \xi_j^\alpha} \mathbf{\Pi} \right) = \mathbf{W}(\xi_v^r) \frac{\partial^\alpha \ell(\xi_v^r)}{\partial \xi_j^\alpha} = \mathbf{W}(\xi_{i < j}) \otimes \mathbf{W}(\xi_j) \frac{d^\alpha \ell(\xi_j)}{d \xi_j^\alpha} \otimes \mathbf{W}(\xi_{i > j}). \quad (5)$$

Eq. (5) closely resembles the stiffness matrix that appears in finite element methods.

Remark 1. *The same algorithm can be used in evaluating the Hadamard product with the surface integral terms in Chan [21, Eq. (58)] by substituting $\alpha = 0$ and the facet cubature nodes in Eq. (4).*

This leads to the main finding of this technical note—for Hadamard products arising in spectral methods that involve some α -th order derivative of a polynomial function, the matrix assembly and evaluation costs dn^{d+1} flops each.

Theorem 2.1. *If the basis function is represented as a tensor product, then the Hadamard product involving some α -th order derivative of the basis function costs dn^{d+1} flops.*

Proof. Consider we have a basis χ evaluated on a cubature set ξ_v^r , and we wish to compute $\left(\frac{\partial \chi(\xi_v^r)}{\partial \xi_j^\alpha} \Pi\right) \circ C$. From Zwanenburg and Nadarajah [29, Proposition 2.1 and Corollary 2.2], we can apply a basis transformation on both C and $\frac{\partial \chi(\xi_v^r)}{\partial \xi_j^\alpha} \Pi$ to a collocated nodal Lagrange set constructed and evaluated on ξ_v^r . It is important to note that for the basis transformation, we can directly use sum-factorization techniques [1] that give an additional dn^{d+1} flops. After the basis transformation, the resulting basis in the Hadamard product is of the form of Eq. (5), and the evaluation of the Hadamard product is of the form of Eq. (3), and thus is evaluated in dn^{d+1} flops. \square

This theorem allows us to solve Hadamard products at $\mathcal{O}(n^{d+1})$ for general uncollocated modal schemes in curvilinear coordinates.

We provide a sample algorithm for implementation in three-dimensions from our in-house PDE solver PHiLiP “Operators” class. A similar structure is done for the surface Hadamard products where the one-dimensional basis matrices are of size $m \times n$, $m < n$. Let’s assume we want to compute $(D \otimes W \otimes W) \circ C_x$, $(W \otimes D \otimes W) \circ C_y$, and $(W \otimes W \otimes D) \circ C_z$, where $W = \text{diag}(w)$ stores some weights, and D is dense. This mimics the Hadamard product to be computed for entropy conserving schemes alike in Chan [21, Eq. (58)]. For the tensor product, we let the x -direction run fastest, then the y -direction, and the z -direction runs slowest. We will refer to the first term as the first direction, the second term as the second direction and the third term as the third direction. We evaluate it in three steps. First, we create two vectors of size $\mathbb{R}^{n^{d+1} \times d}$ storing a sparsity pattern: one stores the non-zero row indices and the other stores the non-zero column indices for each of the d directions. From these, we can build an $n^d \times n$ -sized matrix, for example both $D \otimes W \otimes W$ and C_x , storing only the non-zero entries of the general $n^d \times n^d$ -sized matrix for each of the d directions. We provide the pseudocode algorithm to build $D \otimes W \otimes W$, $W \otimes D \otimes W$, and $W \otimes W \otimes D$. Lastly, after both matrices of size $\mathbb{R}^{n^d \times n}$ for each direction are built, we evaluate the Hadamard product directly.

We generate the sparsity patterns by the algorithm 1:

Algorithm 1 Sparsity Pattern Algorithm

```
1: Create rows and columns vectors of size  $n^{d+1} \times d$  storing the sparsity pattern.
2: Loop over the  $n^4$  indices.
3: for  $i = 0; i < n; i++$  do
4:   for  $j = 0; j < n; j++$  do
5:     for  $k = 0; k < n; k++$  do
6:       for  $l = 0; l < n; l++$  do
7:         Store the array indices and the non-zero row indices.
8:          $\text{array\_index} \leftarrow i * n^3 + j * n^2 + k * n + l$ 
9:          $\text{row\_index} \leftarrow i * n^2 + j * n + k$ 
10:         $\text{rows}[\text{array\_index}][0,1,2] \leftarrow \text{row\_index}$ 
11:        Store the non-zero column indices through pivoting.
                                                     $\triangleright$  Direction 0 (x).
12:         $\text{column\_index\_x} \leftarrow i * n^2 + j * n + l$ 
13:         $\text{columns}[\text{array\_index}][0] \leftarrow \text{column\_index\_x}$ 
                                                     $\triangleright$  Direction 1 (y).
14:         $\text{column\_index\_y} \leftarrow l * n + k + i * n^2$ 
15:         $\text{columns}[\text{array\_index}][1] \leftarrow \text{column\_index\_y}$ 
                                                     $\triangleright$  Direction 2 (z).
16:         $\text{column\_index\_z} \leftarrow l * n^2 + k + j * n$ 
17:         $\text{columns}[\text{array\_index}][2] \leftarrow \text{column\_index\_z}$ 
18:      end for
19:    end for
20:  end for
21: end for
```

Then, using the sparsity patterns, we create the matrices $D \otimes W \otimes W$, $W \otimes D \otimes W$, and $W \otimes W \otimes D$ by the algorithm 2:

where “basis” refers to D in the given direction, “weights” refers to W , and “Basis_Sparse” refers to their tensor product storing only the n^{d+1} non-zero values. We can similarly construct C_x , C_y and C_z using the sparsity patterns. The third step of evaluating the Hadamard product doesn’t require the sparsity patterns since it is the Hadamard product of $\mathbb{R}^{n^d \times n}$ dense matrices.

3. Results

For numerical verification, we use the open-source Parallel High-order Library for PDEs (PHiLiP, <https://github.com/dougshidong/PHiLiP.git>) [28], developed at the Computational Aerodynamics Group at McGill University. For the first test, we consider three-dimensions. We let $(C)_{ij} = c_i c_j$, with $c = \text{rand}([1e^{-8}, 30])$. We compare the cost of evaluating the three-dimensional Hadamard product $\sum_{j=1}^3 \frac{\partial t(\xi_j)}{\partial \xi_j} \circ C$ directly, and using our proposed algorithm in Eq. (3), for polynomial degrees $n \in [3, 15]$.

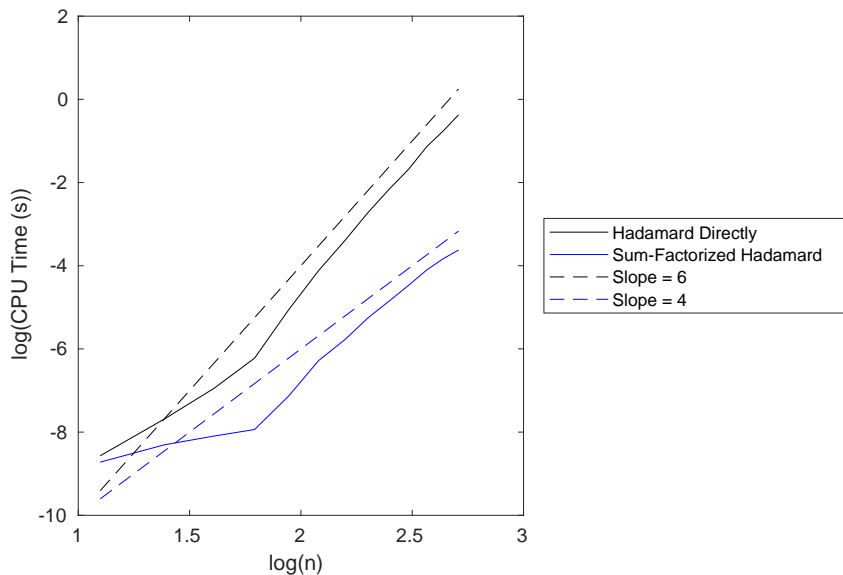


Figure 1: CPU time versus polynomial degree

In Fig. 1, the black solid line corresponds to evaluating the Hadamard directly, the black dashed line corresponds to a slope of 6, the blue solid line corresponds to our proposed method using the tensor-product

Algorithm 2 Basis Assembly Algorithm

```
1: Loop over the  $n^4$  indices.
2: for index=0, counter=0; index <  $n^{d+1}$ ; index++, counter++ do
3:   if counter == n then
4:     counter ← 0
5:   end if
6:   Extract the one-dimensional basis values from the sparsity patterns.
      ▶ We use integer division and % as the mod operator.
7:   x_row_index ← rows[index][0] % n
8:   x_column_index ← columns[index][0] % n
9:   y_row_index ← (rows[index][1] / n) % n
10:  y_column_index ← (columns[index][1] / n) % n
11:  z_row_index ← rows[index][2] / n / n
12:  z_column_index ← columns[index][2] / n / n
      ▶ Basis_Sparse is an array of matrices of size  $d \times (n^d \times n)$ .
13:  Create the matrix storing only non-zero values.
      ▶ Direction 0 (x).
14:  Basis_Sparse[0][rows[index][0]][counter] ← basis[x_row_index][x_column_index] *
      weights[y_row_index] * weights[z_row_index];
      ▶ Direction 1 (y).
15:  Basis_Sparse[1][rows[index][1]][counter] ← basis[y_row_index][y_column_index] *
      weights[x_row_index] * weights[z_row_index];
      ▶ Direction 2 (z).
16:  Basis_Sparse[2][rows[index][2]][counter] ← basis[z_row_index][z_column_index] *
      weights[x_row_index] * weights[y_row_index];
17: end for
```

structure, and the blue dashed line corresponds to a slope of 4. We store the CPU time by running the test on one processor and we record the clock time before the algorithm then subtract the clock time after computing $\sum_{j=1}^3 \frac{\partial f(\xi_j^v)}{\partial \xi_j} \circ C$. In Fig. 1, the conventional way of computing a Hadamard product in all three directions in three-dimensions costs $\mathcal{O}(n^{2d})$, whereas our proposed “sum-factorized” form that exploits the tensor product structure costs $\mathcal{O}(n^{d+1})$.

Next, using our proposed sum-factorized Hadamard product, we wish to compare the performance of the entropy-conserving scheme with the conservative DG scheme using sum-factorization techniques. We solve the three-dimensional inviscid Taylor-Green vortex (TGV) problem on a coarse curvilinear grid using NSFR on uncollocated Gauss-Legendre quadrature nodes. We solve it in six different ways. First, with the conservative DG scheme that does not require a Hadamard product. Second, the conservative DG scheme over-integrated by $2(p + 1)$ to resemble exact integration for a cubic polynomial on a curvilinear grid. We consider over-integration because it is another tool used for stabilization [30] through polynomial dealiasing. Lastly, with our NSFR entropy conserving scheme [25, 26] that requires an uncollocated Hadamard product along with entropy projection techniques [22]. We then, in dashed lines, run the same tests with an FR correction value of c_+ [31] to compare the additional cost of FR versus its DG equivalent. For the test, we perform 10 residual solves sequentially and record the total CPU time for the 10 residual solves.

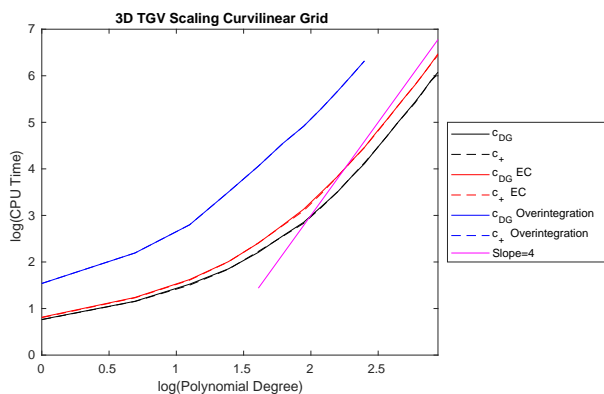


Figure 2: CPU time versus polynomial degree TGV

From Figure 2, all three methods have the solver scale at order $\mathcal{O}(p^{d+1})$ in curvilinear coordinates because they exploit sum-factorization [1] for the matrix-vector products, and the NSFR-EC scheme uses our proposed sum-factorized Hadamard product evaluation. The blue line representing the over-integrated conservative DG scheme took the most amount of time, and the cut-off at extremely high polynomial orders,

$p > 20$, was due to memory issues with storing the additional quadrature nodes. The conservative DG scheme took the least amount of time, but the entropy conserving scheme involving the Hadamard product with the two-point flux had a comparable CPU time thanks to the algorithm presented in Section 2. Also, there was a negligible computational cost difference between all c_{DG} versus c_+ schemes since the mass matrix inverse was approximated in a weight-adjusted form. From Fig. 2, it appears that using the algorithm in Sec. 2, the entropy conserving scheme’s cost is more comparable to the conservative DG scheme rather than an over-integrated/exactly integrated DG scheme.

To further demonstrate the performance differences between the NSFR-EC-DG scheme using the “sum-factorized” Hadamard product evaluations detailed in Sec. 2 and the conservative DG scheme in curvilinear coordinates, we run the inviscid TGV on a non-symmetrically warped curvilinear grid and compare the wall clock times. All schemes use an uncollocated, modal Lagrange basis, and are integrated on Gauss-Legendre quadrature nodes. We integrate in time with a 4-*th* order Runge-Kutta time-stepping scheme with an adaptive Courant-Friedrichs-Lewy value of 0.1 until a final time of $t_f = 14$ s. For NSFR-EC-DG we use Chandrashekar’s flux [32] in the volume and surface with Ranocha’s pressure fix [33]. For the DG conservative scheme, we use the Roe [34] surface numerical flux. All of the tests were run on a single node provided by the Digital-Alliance of Canada.

Table 1: TGV Wall Clock Time

p	Number of Elements	Scheme	Wall Clock (s)
3	4^3	NSFR-EC-DG	718.35
		DG-cons	604.15
		DG-cons-overint	2508.57
	8^3	NSFR-EC-DG	5441.31
		DG-cons	6040.61
		DG-cons-overint	23280.30
4	4^3	NSFR-EC-DG	1790.95
		DG-cons	1495.61
		DG-cons-overint	5955.21
	8^3	NSFR-EC-DG	9259.31
		DG-cons	8090.78
		DG-cons-overint	28198.60
5	4^3	NSFR-EC-DG	1617.21
		DG-cons	crashed
		DG-cons-overint	11055.10
	8^3	NSFR-EC-DG	12050.60
		DG-cons	crashed
		DG-cons-overint	33741.20

From Table 1, the NSFR-EC-DG scheme took about a 11% longer run time as compared to conservative DG. This small percentage difference demonstrates how the algorithm in Sec. 2 has drastically reduced the computational cost of computing a two-point flux, since we are not required to do twice nor squared the work. The $p = 5$ DG conservative scheme diverged at $t = 9.06$ s with a wall clock time of 1369.93 s on the 4^3 mesh, and at $t = 6.70$ s with a wall clock of 4473.26 s on the 8^3 mesh. This further demonstrates the advantage of the NSFR-EC scheme since it has provable guaranteed nonlinear stability for a reasonable computational cost trade-off. The over-integrated scheme took on average 396% longer run-time than the NSFR-EC-DG scheme. From both Fig. 2 and Table 1, it is clear that with the proposed sum-factorized

Hadamard product, entropy conserving and stable methods are computationally competitive with classical DG schemes.

4. Conclusion

We derived and demonstrated a “sum-factorized” technique to build and compute Hadamard products at $\mathcal{O}(n^{d+1})$. With the fast evaluations, the computational cost of entropy conserving and stable schemes becomes computationally competitive with the classical conservative modal discontinuous Galerkin method in general three-dimensional curvilinear coordinates.

References

- [1] S. A. Orszag, Spectral methods for problems in complex geometrics, in: Numerical methods for partial differential equations, Elsevier, 1979, pp. 273–305.
- [2] E. Tadmor, Skew-self adjoint form for systems of conservation laws, *Journal of Mathematical Analysis and Applications* 103 (1984) 428–442.
- [3] T. C. Fisher, M. H. Carpenter, High-order entropy stable finite difference schemes for nonlinear conservation laws: Finite domains, *Journal of Computational Physics* 252 (2013) 518–557.
- [4] T. C. Fisher, M. H. Carpenter, J. Nordström, N. K. Yamaleev, C. Swanson, Discretely conservative finite-difference formulations for nonlinear conservation laws in split form: Theory and boundary conditions, *Journal of Computational Physics* 234 (2013) 353–375.
- [5] T. C. Fisher, High-order L2 stable multi-domain finite difference method for compressible flows, Ph.D. thesis, Purdue University, 2012.
- [6] M. H. Carpenter, T. C. Fisher, E. J. Nielsen, S. H. Frankel, Entropy stable spectral collocation schemes for the Navier–Stokes equations: Discontinuous interfaces, *SIAM Journal on Scientific Computing* 36 (2014) B835–B867.
- [7] M. Parsani, M. H. Carpenter, E. J. Nielsen, Entropy stable discontinuous interfaces coupling for the three-dimensional compressible Navier-Stokes equations., *J. Comput. Phys.* 290 (2015) 132–138.

- [8] M. Parsani, M. H. Carpenter, E. J. Nielsen, Entropy stable wall boundary conditions for the three-dimensional compressible Navier–Stokes equations, *Journal of Computational Physics* 292 (2015) 88–113.
- [9] M. Parsani, M. H. Carpenter, T. C. Fisher, E. J. Nielsen, Entropy stable staggered grid discontinuous spectral collocation methods of any order for the compressible Navier–Stokes equations, *SIAM Journal on Scientific Computing* 38 (2016) A3129–A3162.
- [10] M. H. Carpenter, M. Parsani, E. J. Nielsen, T. C. Fisher, Towards an entropy stable spectral element framework for computational fluid dynamics, in: *54th AIAA Aerospace Sciences Meeting*, 2016, p. 1058.
- [11] N. K. Yamaleev, M. H. Carpenter, A family of fourth-order entropy stable nonoscillatory spectral collocation schemes for the 1-D Navier–Stokes equations, *Journal of Computational Physics* 331 (2017) 90–107.
- [12] J. Crean, J. E. Hicken, D. C. Del Rey Fernández, D. W. Zingg, M. H. Carpenter, Entropy-stable summation-by-parts discretization of the Euler equations on general curved elements, *Journal of Computational Physics* 356 (2018) 410–438.
- [13] T. Chen, C.-W. Shu, Entropy stable high order discontinuous Galerkin methods with suitable quadrature rules for hyperbolic conservation laws, *Journal of Computational Physics* 345 (2017) 427–461.
- [14] D. C. Del Rey Fernández, J. Crean, M. H. Carpenter, J. E. Hicken, Staggered-grid entropy-stable multi-dimensional summation-by-parts discretizations on curvilinear coordinates, *Journal of Computational Physics* 392 (2019) 161–186.
- [15] L. Friedrich, G. Schnücke, A. R. Winters, D. C. Del Rey Fernández, G. J. Gassner, M. H. Carpenter, Entropy stable space–time discontinuous Galerkin schemes with summation-by-parts property for hyperbolic conservation laws, *Journal of Scientific Computing* 80 (2019) 175–222.
- [16] G. J. Gassner, A skew-symmetric discontinuous Galerkin spectral element discretization and its relation to SBP-SAT finite difference methods, *SIAM Journal on Scientific Computing* 35 (2013) A1233–A1253.

- [17] G. J. Gassner, A. R. Winters, D. A. Kopriva, Split form nodal discontinuous Galerkin schemes with summation-by-parts property for the compressible Euler equations, *Journal of Computational Physics* 327 (2016) 39–66.
- [18] H. Ranocha, P. Öffner, T. Sonar, Summation-by-parts operators for correction procedure via reconstruction, *Journal of Computational Physics* 311 (2016) 299–328.
- [19] H. Ranocha, P. Öffner, T. Sonar, Extended skew-symmetric form for summation-by-parts operators and varying Jacobians, *Journal of Computational Physics* 342 (2017) 13–28.
- [20] Y. Abe, I. Morinaka, T. Haga, T. Nonomura, H. Shibata, K. Miyaji, Stable, non-dissipative, and conservative flux-reconstruction schemes in split forms, *Journal of Computational Physics* 353 (2018) 193–227.
- [21] J. Chan, On discretely entropy conservative and entropy stable discontinuous Galerkin methods, *Journal of Computational Physics* 362 (2018) 346–374.
- [22] J. Chan, Skew-symmetric entropy stable modal discontinuous Galerkin formulations, *Journal of Scientific Computing* 81 (2019) 459–485.
- [23] J. Chan, L. C. Wilcox, On discretely entropy stable weight-adjusted discontinuous Galerkin methods: Curvilinear meshes, *Journal of Computational Physics* 378 (2019) 366–393.
- [24] J. Chan, D. C. Del Rey Fernández, M. H. Carpenter, Efficient entropy stable gauss collocation methods, *SIAM Journal on Scientific Computing* 41 (2019) A2938–A2966.
- [25] A. Cicchino, S. Nadarajah, D. C. Del Rey Fernández, Nonlinearly stable flux reconstruction high-order methods in split form, *Journal of Computational Physics* (2022) 111094.
- [26] A. Cicchino, D. C. Del Rey Fernández, S. Nadarajah, J. Chan, M. H. Carpenter, Provably stable flux reconstruction high-order methods on curvilinear elements, *Journal of Computational Physics* 463 (2022) 111259.
- [27] H. Ranocha, M. Schlottke-Lakemper, J. Chan, A. M. Rueda-Ramírez, A. R. Winters, F. Hindenlang, G. J. Gassner, Efficient implementation of modern entropy stable and kinetic energy preserving discontinuous Galerkin methods for conservation laws, *arXiv preprint arXiv:2112.10517* (2021).

- [28] D. Shi-Dong, S. Nadarajah, Full-space approach to aerodynamic shape optimization, *Computers & Fluids* (2021) 104843.
- [29] P. Zwanenburg, S. Nadarajah, Equivalence between the energy stable flux reconstruction and filtered discontinuous Galerkin schemes, *Journal of Computational Physics* 306 (2016) 343–369.
- [30] A. R. Winters, R. C. Moura, G. Mengaldo, G. J. Gassner, S. Walch, J. Peiro, S. J. Sherwin, A comparative study on polynomial dealiasing and split form discontinuous Galerkin schemes for under-resolved turbulence computations, *Journal of Computational Physics* 372 (2018) 1–21.
- [31] P. Vincent, P. Castonguay, A. Jameson, Insights from von Neumann analysis of high-order flux reconstruction schemes, *Journal of Computational Physics* 230 (2011) 8134–8154.
- [32] P. Chandrashekar, Kinetic energy preserving and entropy stable finite volume schemes for compressible Euler and Navier-Stokes equations, *Communications in Computational Physics* 14 (2013) 1252–1286.
- [33] H. Ranocha, G. J. Gassner, Preventing pressure oscillations does not fix local linear stability issues of entropy-based split-form high-order schemes, *Communications on Applied Mathematics and Computation* 4 (2022) 880–903.
- [34] P. L. Roe, Approximate Riemann solvers, parameter vectors, and difference schemes, *Journal of computational physics* 43 (1981) 357–372.